

## Ultrahigh-vacuum scanning force microscopy: Atomic-scale resolution at monatomic cleavage steps

L. Howald, H. Haefke, R. Lüthi, E. Meyer, G. Gerth,\* H. Rudin, and H.-J. Güntherodt  
*Institute of Physics, University of Basel, Klingelbergstrasse 82, CH-4056 Basel, Switzerland*

(Received 8 September 1993)

The surfaces of *in situ* cleaved NaF crystals have been studied by scanning force microscopy (SFM) in ultrahigh vacuum (UHV). Operating the UHV force microscope in the contact mode, the surface structure with extended terraces interrupted by steps of typically 0.25 nm and 0.5 nm in height is revealed. Atomic-scale resolution is achieved on the terraces as well as at monatomic steps of the ionic crystal. The square surface lattice shows a periodicity of  $0.45 \pm 0.04$  nm that corresponds well to the spacing between equally charged ions along the  $\langle 100 \rangle$  directions in the bulk phase. From the SFM data at cleavage steps the imaging area of the sensing tip is estimated to be less than  $1 \text{ nm}^2$ . Some aspects of the contrast mechanism in the lateral and normal force images are discussed. The SFM data are complemented by low-energy-electron-diffraction measurements on NaF(001) carried out in the same compact UHV system.

### I. INTRODUCTION

Scanning force microscopy (SFM) offers the capability for investigating solid surfaces, rendering information from the micrometer scale to the subnanometer scale. In contrast to the scanning tunneling microscope, which detects a tunneling current between probing tip and electrically conducting sample, the scanning force microscope can be operated on insulating samples. The range of samples investigated by SFM includes to date inorganic and organic materials, as well as technological samples. The surfaces of insulators, in particular of ionic crystals, are of considerable current interest both in scientific and in technological fields. Owing to the rigidity of many ionic crystals, clean surfaces can be obtained by a simple cleavage procedure. To study surface properties by SFM and to understand the imaging and contrast mechanisms, the samples should be prepared and probed in a well-defined environment and at constant conditions. These prerequisites are fulfilled in an ultrahigh vacuum (UHV).

Although force microscopes have been adapted for a wide variety of environments, there are only few publications on SFM measurements in UHV. The first uses of SFM in UHV were published by Meyer and Amer<sup>1,2</sup> and by Neubauer *et al.*<sup>3</sup> The former group has reported on UHV measurements of NaCl(001) surfaces prepared by *ex situ* cleavage and subsequent thermal etching in UHV. They observed in step-free areas, i.e., on terraces, a regular atomic lattice reflecting the cubic structure of the NaCl crystal. Scanning across topological features, e.g., surface steps, they found direction-dependent lateral forces. Atomic-scale friction of diamond on diamond has been studied by Germann *et al.*<sup>4</sup> with a UHV force microscope. The surface of KBr(001), obtained by *in situ* cleavage, has been probed by SFM by Giessibl and Binnig<sup>5</sup> at low temperatures in UHV. The authors obtained SFM images of the periodic arrangement of sur-

face atoms as well as one image of a cleavage step at atomic-scale resolution.<sup>6</sup> The interesting question how far the lateral resolution of SFM can be pushed for non-periodic structures seems to be quite delicate. Atomic defects, such as cleavage steps of ionic crystals, offer the possibility to answer this question at least in one dimension perpendicular to the step. Very recently, Ohnesorge and Binnig<sup>7</sup> have observed atomic-scale resolution along monatomic steps of CaCO<sub>3</sub> by SFM in liquid environment (water).

In this work we report on UHV measurements on (001) surfaces of NaF at room temperature. The orientation and structural quality of the NaF cleavage faces are examined by low-energy electron diffraction (LEED). The surface and lattice structures of NaF(001) are imaged by the force microscope which is operated in the contact mode. Reproducible atomic-scale resolution is achieved on terraces and at cleavage steps. By examining the extent of the imaged step regions, an upper limit of the contact area can be given for the SFM tip.

### II. EXPERIMENTAL DETAILS

The SFM studies were performed at room temperature under UHV conditions ( $5 \times 10^{-11}$  mbar). The force microscope is part of a compact UHV system consisting of the SFM chamber, an analysis chamber, and a preparation chamber. As described earlier,<sup>8</sup> the instrument design uses an optical beam deflection detector with a four-quadrant photodiode. Thus, it is possible to detect simultaneously the normal and lateral (frictional) forces. The normal force is measured by the deflection of the cantilever-type spring normal to the sample surface. From the torsion of the cantilever, the lateral force (acting parallel to the surface) is determined. Commercially available silicon cantilevers with integrated tips were used as force sensors. Their spring constants varied between

0.4 and 0.6 N/m.<sup>9</sup> The tips were coated with a 8 nm aluminum film oxidized in air. The calibration of the force microscope in terms of lateral and vertical distances was performed with stepped Si(111) 7×7 at which the instrument was operated in the scanning tunneling mode.<sup>8</sup>

The used NaF crystals were obtained by cutting from a large Czochralski single crystal grown in a dry nitrogen atmosphere. NaF crystallizes with the NaCl-type structure and shows perfect cleavability parallel to the {100} faces. Its unit cell length  $a_0$  is 0.462 nm.<sup>10</sup> The cleavage was carried out in the preparation chamber at room temperature and at a pressure of  $8 \times 10^{-11}$  mbar. Then the crystal was transferred either to the analysis chamber equipped with a combined LEED/Auger electron optics or to the SFM chamber. Order properties of the NaF(001) face were determined by means of the four-grid LEED system (Omicron Vakuumphysik GmbH). Being placed in the SFM sample holder, the crystal was approached to the silicon cantilever. During approaching, a strong attractive interaction between tip and cantilever was observed and estimated to be of the order of  $\mu\text{N}$ . This long-range force originates from the NaF cleavage face which is, after cleavage, in general patchwise electrically charged, both positively and negatively.<sup>11,12</sup> For NaF cleavage faces, charge densities of patches (about 1 mm<sup>2</sup> in size) up to about  $8 \times 10^{-9}$  C/cm<sup>2</sup> have been measured.<sup>12</sup>

Just after approaching into contact, a large repulsive force was observed in the contact region between tip and sample. This short-range force resulted from balancing the attractive long-range electrostatic and van der Waals forces acting on the whole tip. For the scanning process, we have reduced this large force to a few nN by carefully retracting the cantilever spring close to the point where the tip jumps off the sample surface. The imaging quality was reproducible over several days and for all tips used. It should be noted that the electrostatic attraction due to surface charges was present during four days. Only after heating the NaF crystal for several minutes at 450 °C was the electrostatic force reduced to the order of  $10^{-8}$  N.

### III. RESULTS AND DISCUSSION

To determine the orientation of the NaF crystal and to ensure a structurally very good cleavage face, a LEED examination was performed. LEED spectra could be recorded over the energy range from 50 to 85 eV. The intensity of the primary electron beam ejected from the LEED gun was varied between 1.0 and 2.5  $\mu\text{A}$ . Figure 1 shows a LEED pattern at 78 eV of a freshly prepared NaF cleavage face. The diffraction pattern consists of the spots expected for the perfect NaF(001). As previously reported by McRae and Caldwell,<sup>13</sup> the spot and background patterns correspond to a unit cell mesh identical with that of the unperturbed crystal.

Figure 2 shows a representative force micrograph of a NaF cleavage face. The window size is  $1 \times 1 \mu\text{m}^2$ . The topographic data are obtained at constant normal force. The data are displayed on an arbitrary chosen linear gray scale to indicate the relative height of surface features.

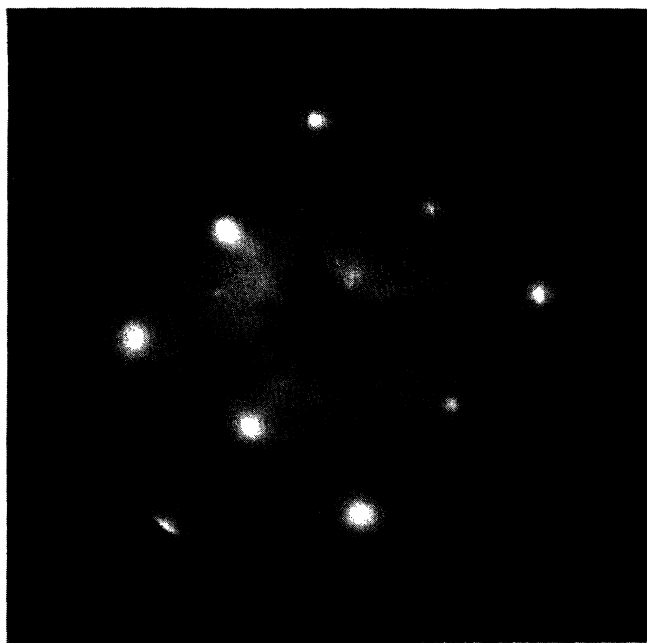


FIG. 1. LEED pattern of NaF(001). Primary electron energy 78 eV.

High features are assigned bright colors and low features dark colors. The surface structure is dominated by many cleavage steps aligned parallel to the [100] direction. The lateral separation between steps, i.e., the terrace width, varies between 50 nm and 1  $\mu\text{m}$ . The majority of steps are determined to be  $0.25 \pm 0.03$  nm or  $0.50 \pm 0.06$  nm in height. Some steps are considerably higher. The smallest

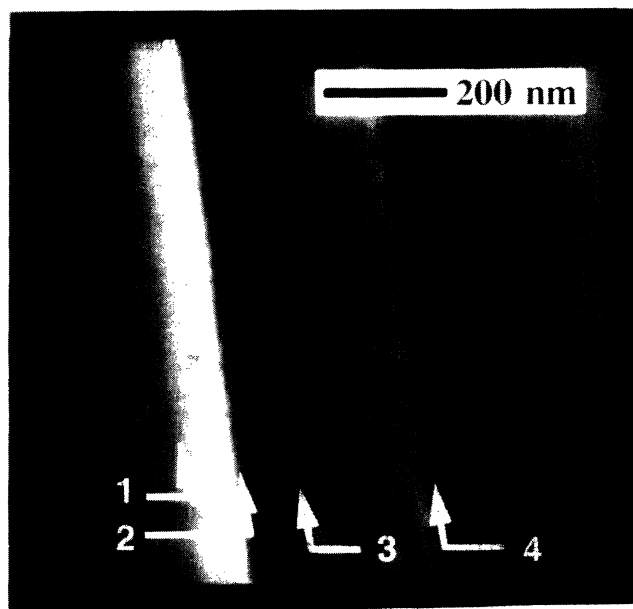


FIG. 2. Force micrograph of a NaF cleavage face on the micrometer scale. The image was taken in the constant force mode. Corresponding to the chosen gray scale, bright regions are assigned high surface features and dark regions low features. The height of several cleavage steps (marked by arrows) were determined to be 0.25 nm (steps 1, 3, and 4) and 0.5 nm (step 2), respectively.

measured step height corresponds well to the expected value of 0.23 nm for monatomic steps; i.e., they are  $a_0/2$  high. Using  $z$ -profile analysis (termed also line section) from left to right, the sense of the steps (ascending or descending) and their mean heights are determined. For example, step 1 is ascending by  $0.25 \pm 0.03$  nm and step 2 is descending by  $0.5 \pm 0.05$  nm. Both steps 3 and 4 are one atom high and their sense is ascending and descending, respectively.

Zooming in terraces, the regular surface lattice of NaF(001) is revealed (Fig. 3). The window size is  $3.4 \times 3.4$  nm<sup>2</sup>. This raw-data image is taken from the lateral force signal of the instrument. Analogous to normal force signals, a linear gray scale is also applied to lateral forces: Here, dark color corresponds to larger values of the lateral force. The contrast difference between bright and dark areas represents a change in the lateral force of  $7 \pm 3$  nN. The SFM image is slightly distorted in the vertical direction (i.e., in slow scan direction) due to thermal drift of the sample with respect to the tip. The direction of drift was almost parallel to the slow scan direction. Therefore, we obtain the most precise data from the fast scan direction (horizontal image direction) which is near the crystallographic [010] direction. The periodicity of lattice features along the [010] direction is determined to be  $0.45 \pm 0.04$  nm. This value is in good agreement with the unit cell length ( $a_0 = 0.462$  nm) and is identical with the spacing between equally charged ions in the bulk lattice; thus the NaF(001) surface is covered by a  $(1 \times 1)$  unreconstruction. Taking into account this fact, we conclude that the force microscope is not equally sensitive to the positive sodium and negative fluorine ions. Only one species is imaged while the other species is depressed. Practically, the same imaging effect on ionic crystal surfaces has been observed by other groups for LiF,<sup>14</sup> NaCl,<sup>2</sup>

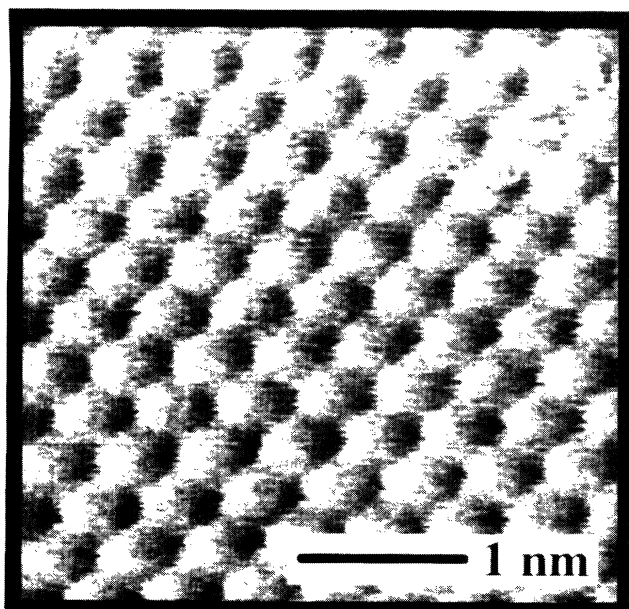


FIG. 3. Atomic-scale resolution on a terrace in the lateral force mode. The spacing between two atomic features (bright spots) in the [010] direction is 0.45 nm and corresponds well to the unit cell length  $a_0$  of 0.463 nm.

and AgBr.<sup>15,16</sup> A comparison of the ionic radii for Na<sup>+</sup> ( $r = 0.116$  nm) and F<sup>-</sup> ( $r = 0.114$  nm) at coordination number six<sup>17</sup> implies that for NaF the different imaging behavior of the cations and anions cannot be explained by a simple hard sphere model.<sup>18</sup>

Simultaneously with the lateral force data, displayed in Fig. 3, we also acquired the normal force data (variable deflection mode). However, the normal force variations are two orders of magnitude smaller and therefore difficult to detect. This fact is still unclear and, to our knowledge, does not originate from an instrumental artifact. The optical detection scheme has even a higher sensitivity for normal forces than for lateral forces. The normal force signal is not presented here because it was so weak that it became comparable to the cross talk between the two channels of the photodetector.

The imaging ability of the force microscope at monatomic surface steps is manifested in Figs. 4 and 5. Figure 4(a) shows the topography image of two terraces interrupted by a monatomic step running along the [100] direction. These data are taken at constant normal force and the scanned area is  $130 \times 130$  nm<sup>2</sup>. The  $z$ -profile analysis, done along the white line in Fig. 4(a), exhibits a step height of 0.25 nm [Fig. 4(b)]. At higher magnifications the topographic signal became more and more diffuse until only a weak image contrast remained. Therefore the force micrographs are taken from the lateral force data that provide images of high contrast. For comparison Fig. 5(a) shows a lateral force image monitored simultaneously with the topographic data of Fig. 4(a). The same step appears here as a sharp, straight line. The white frame superimposed to the step indicates the surface area where the atomic-scale data of Fig. 5(b) was achieved.

The high-resolution SFM image shown in Fig. 5(b), window size  $5.6 \times 5.6$  nm<sup>2</sup>, exhibits both regular surface lattices on the lower terrace (left) and upper terrace (right). They are separated by a narrow diffuse region of 0.5–1 nm width which we attribute to the step region. Following a diagonal row of atomic features on the lower terrace, along the black line in Fig. 5(b), the line runs into a trough between two protrusive rows on the upper terrace. Reversely, the same result is obtained when crossing the step region from right above to left below [see white line in Fig. 5(b)]. This discontinuity in the [110] ion rows at the step is exactly what we expect from a terrace-ledge model of a NaCl-type crystal. As can be seen in Fig. 6, both terraces are covered by alternating black and white rows of ions along  $\langle 110 \rangle$  directions. At the monatomic step, each row of one species is continued by a row of the other species. This is, however, valid at steps that are  $n \times a_0/2$  in height, where  $n$  is odd. The ability of the force microscope to detect the shift of the  $\langle 110 \rangle$  rows at monatomic steps is an evidence for the different sensitivity of the probing tip for cations and anions in UHV. Along the [110] ion rows the discontinuity is less pronounced [Fig. 5(b)]; this cannot be expected from a perfect tip-surface interaction. Therefore, we now discuss briefly the relation between tip geometry and imaging contrast.

From an idealized tip [cf. Fig. 7(a)] an upper limit for

the local radius of curvature can be estimated. The distance  $S$  is the separation between tip apex and the upper edge of the step, having the height  $H$ . Assuming a locally spherical tip, the radius  $R$  becomes  $R = (S^2 + H^2)/2H$ . From the SFM data in Fig. 6(b),  $S$  is taken to 1 nm, corresponding to the width of the diffuse step region. For  $H=0.25$  nm, the resulting local radius of curvature is 2.1 nm or less. A more realistic tip shape is sketched in Fig. 7(b). This tip exhibits a flat contact region with an extent that is comparable to  $S$ . Additionally, the tip has an average radius of curvature that is considerably

larger than the above estimated local value. Assuming a circular contact area with 1 nm diameter and a repulsive force of 5 nN, the mean pressure onto this surface is about 6 GPa. For a given repulsive force this large value can only be reduced by assuming a noncircular contact area which has its longer extent along the direction of step edges. Although there is no direct evidence for an asymmetric tip in our data, the formation of such a tip

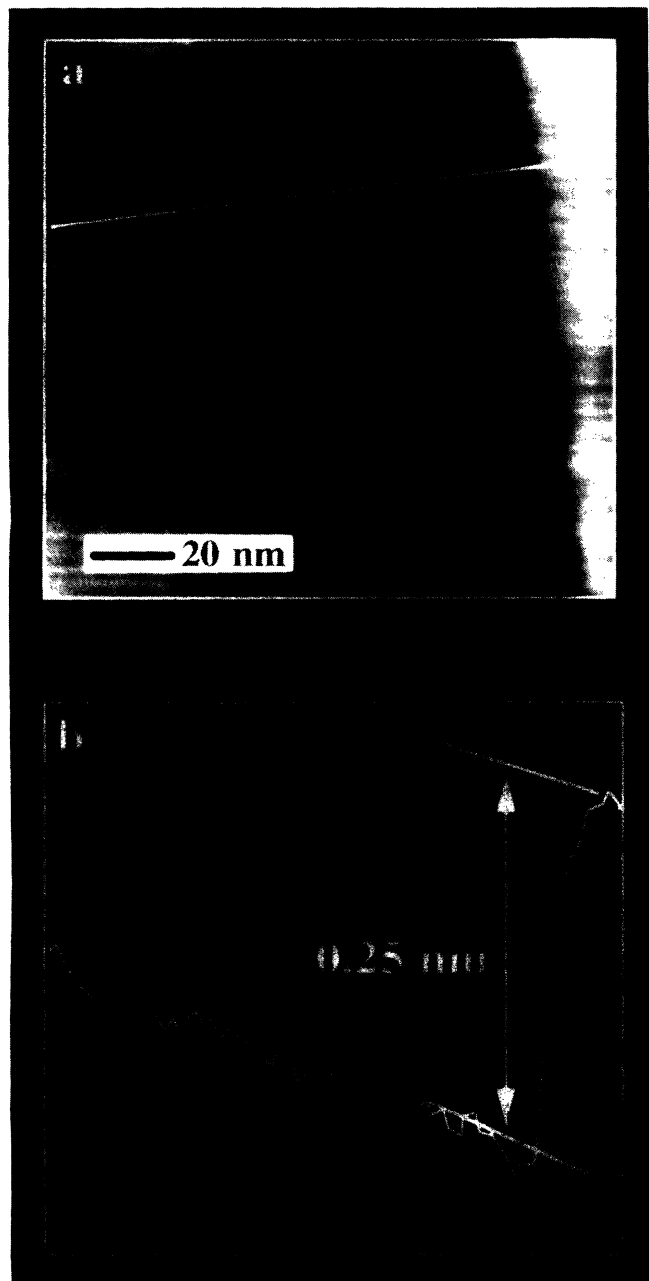


FIG. 4. (a) Topographic image of a monatomic step taken in the constant force mode. (b) The  $z$ -profile analysis (line section) taken along the white line in (a) reveals the step height of 0.25 nm.

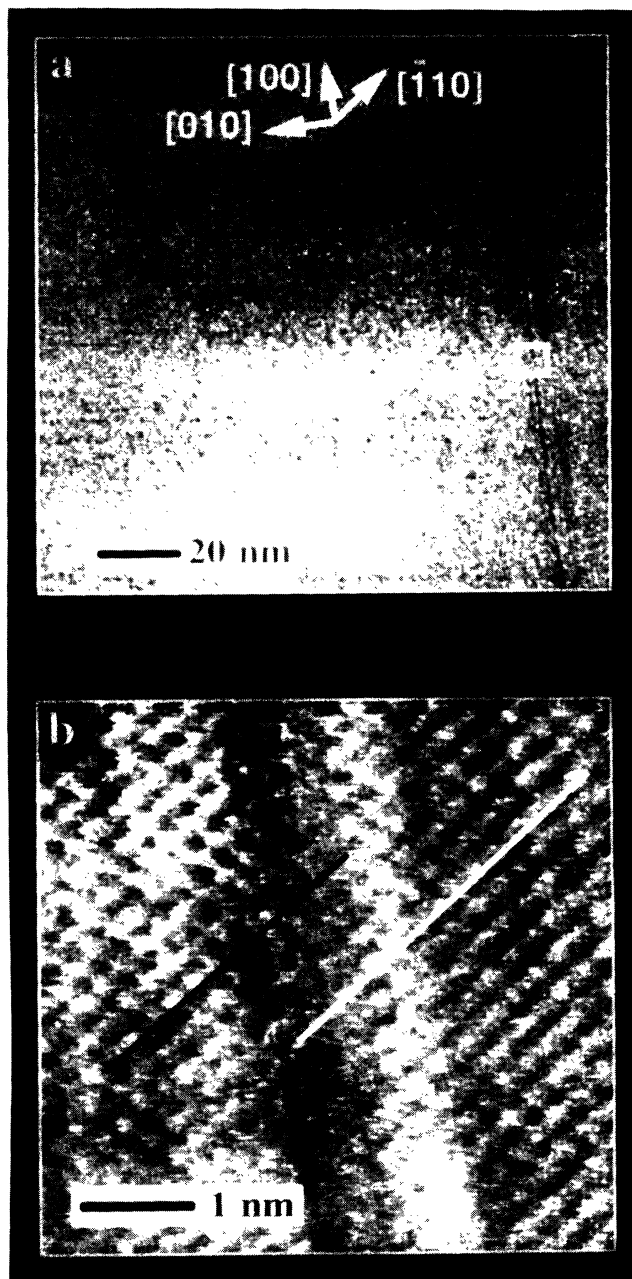


FIG. 5. (a) Lateral force data taken simultaneously with the topographical data of Fig. 4(a). The monatomic step appears here as sharp line. (b) Atomic-scale resolution along this cleavage step in  $5.6 \times 5.6$  nm<sup>2</sup> surface area marked by the white frame in (a). The regular lattice patterns are separated by a diffuse region of 0.5 to 1 nm width. The white and black solid lines indicate the shift of atomic rows between adjacent terraces.

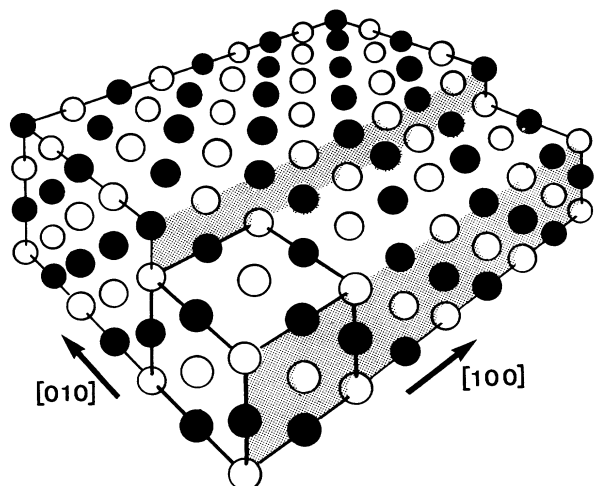


FIG. 6. Perspective view of a terrace-ledge model of a NaCl-type crystal. Both ionic species, represented by open and solid circles, build up two interpenetrating face-centered-cubic lattices. The outline of a single unit cell is indicated by solid lines at the front corner.

shape can be thought to result from the repeated scan over step edges.

Due to the small tip-sample contact area, the local pressure and shear stress can reach the limit at which deformation occurs. Some mechanisms of material deformation were proposed in the literature on scanning force and scanning tunneling microscopy.<sup>19</sup> A shear process within the {100} planes of NaF is very improbable because the primary glide system in NaCl-type crystals is {110}<110>.<sup>20</sup> Gliding on other low-index planes would need enormous forces for juxtaposing equally charged ions. Most probably, the tip apex consists in our case of an amorphous layer of aluminum oxide. A destructive interaction would result in abrasion of the tip or/and scratching of the NaF surface during the scan process. None of these facts was observed in our measurements.

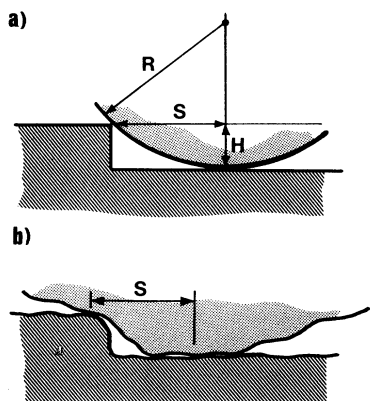


FIG. 7. (a) Idealized tip with a local radius of curvature  $R$  at a step of height  $H$ . For a given separation  $S$  and height  $H$  the radius  $R$  can be calculated. (b) A more realistic tip with a prominent feature and a flat contact area in the nanometer range.

A further example for the nonideal image behavior of the used tip is shown in Fig. 8. The lateral force data were taken while scanning across a biatomic step (step 2 in Fig. 3). The scan direction is from left to right at which the probing tip runs downward. At this step, a 6-nm-wide diffuse region is observed where the atomic structures of sample and tip are folded. Using again the above formula for the local radius of curvature, we calculate the tip radius to  $R = 36$  nm. This comparatively large value indicates that the data of Fig. 6 were obtained with a very small prominent tip feature consisting of only a few atoms. Nevertheless, the imaging quality was very stable and similar images were taken at more than 20 different locations on various cleavage steps.<sup>21</sup>

The force interaction between tip and sample can be composed of several contributions, such as electrostatic, van der Waals, short-range repulsive, and frictional forces. There are some calculations for ionic crystals. For example, Girard *et al.*<sup>22</sup> have modeled the van der Waals forces between a tungsten tip and a NaCl(001) surface. These forces can be split into a larger part that does not depend on the lateral position over the sample and a smaller part that varies with the lateral position. The variable van der Waals contribution is found to be different for the anion and cation sites.

Giessibl<sup>23</sup> has discussed an electrostatic imaging model for a nonconducting tip above the surface of an ionic crystal. The electric field of the ionic sample induces a polarization in the tip. In this model the resulting normal force, acting on the tip, is identical above cation and anion sites. Thus, the lateral periodicity is half the distance than for the van der Waals forces. The author has calculated the force exerted on an oxygen atom above the surface of KBr(001). For different lateral positions of the probing atom along a straight line above two surface atoms, he obtained a cosinelike dependence of the normal force (full amplitude above ionic sites). We have used the

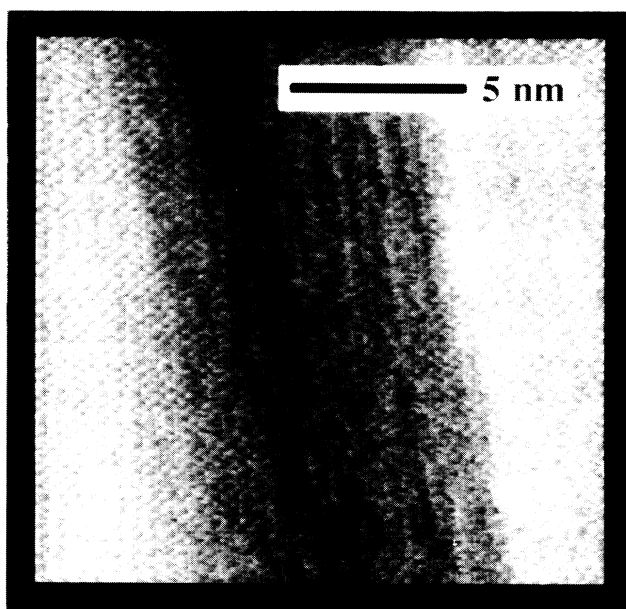


FIG. 8. Lateral force image at the step 2 of Fig. 2. The diffuse region at this 0.5 nm step is about 6 nm wide.

same relations to calculate also the lateral force dependence for an oxygen atom above the NaF(001) surface. The calculation provides a sinelike lateral force variation with comparable amplitude and with the same periodicity as the normal force variation. Consequently, the measured image contrast on NaF(001) with a different periodicity and much larger force variations cannot be described by this latter model.

In addition to the model of Girard *et al.*<sup>22</sup> the correct periodicity can also be obtained with a permanently polarized or charged tip. Further calculations have to be done in the near future, especially to understand the very large difference between normal and lateral forces observed in the UHV measurements.

In conclusion, our UHV force microscope has shown

atomic-scale resolution at cleavage steps of NaF(001) in a reproducible manner. Out of the lateral force data, the shape of the realistic tip could be discussed by means of simple geometrical considerations. The large difference between normal and lateral force variations is not yet understood and is the subject of ongoing work.

#### ACKNOWLEDGMENTS

We wish to thank H. Stenzel for providing the crystal material. This work was supported by the Swiss National Science Foundation (NFP 24) and the Kommission zur Förderung der wissenschaftlichen Forschung.

\* Permanent address: Max Planck Institute of Microstructure Physics, Weinberg 2, D-06120 Halle (Saale), FRG.

<sup>1</sup> G. Meyer and N.M. Amer, *Appl. Phys. Lett.* **53**, 1045 (1988); **53**, 2400 (1988).

<sup>2</sup> G. Meyer and N.M. Amer, *Appl. Phys. Lett.* **56**, 2100 (1990); **57**, 2089 (1990).

<sup>3</sup> G. Neubauer, S.R. Cohen, G.M. McClelland, D. Horne, and C.M. Mate, *Rev. Sci. Instrum.* **61**, 2296 (1990).

<sup>4</sup> G.J. Germann, S.R. Cohen, G. Neubauer, G.M. McClelland, H. Seki, and D. Coulman, *J. Appl. Phys.* **73**, 163 (1993).

<sup>5</sup> F.J. Giessibl and G. Binnig, *Ultramicroscopy* **42-44**, 281 (1992).

<sup>6</sup> F.J. Giessibl, Ph.D. thesis, Ludwig Maximilians University, Munich, 1991.

<sup>7</sup> F. Ohnesorge and G. Binnig, *Science* **260**, 1451 (1993).

<sup>8</sup> L. Howald, E. Meyer, R. Lüthi, H. Haefke, R. Overney, H. Rudin, and H.-J. Güntherodt, *Appl. Phys. Lett.* **63**, 117 (1993).

<sup>9</sup> Nano Sensors Dr. Olaf Wolter GmbH, Wachholderweg 8, D-7042 Aidlingen 3, Germany.

<sup>10</sup> *Inorganic Compounds*, edited by J.D.H. Donnay and H.M. Ondik, Natl. Bur. Stand. (U.S. GPO, Washington, D.C., 1973).

<sup>11</sup> G.I. Distler, E.I. Kortukova, and S.A. Kobzoreva, *Krist. Tech.* **8**, 67 (1973).

<sup>12</sup> J. Wollbrandt, E. Linke, and U. Brücker, *Exp. Tech. Phys.* **23**, 65 (1975).

<sup>13</sup> E.G. McRae and C.W. Caldwell, *Surf. Sci.* **7**, 41 (1967).

<sup>14</sup> E. Meyer, H. Heinzlmann, H. Rudin, and H.-J. Güntherodt, *Z. Phys. B* **79**, 3 (1991).

<sup>15</sup> E. Meyer, H.-J. Güntherodt, H. Haefke, G. Gerth, and M. Krohn, *Europhys. Lett.* **15**, 319 (1991); H. Haefke, E. Meyer, H.-J. Güntherodt, G. Gerth, and M. Krohn, *J. Imag. Sci.* **35**, 290 (1991).

<sup>16</sup> H. Haefke, E. Meyer, L. Howald, U. Schwarz, G. Gerth, and M. Krohn, *Ultramicroscopy* **42-44**, 290 (1992).

<sup>17</sup> F.A. Cotton and G. Wilkinson, *Advanced Inorganic Chemistry*, 5th ed. (Wiley, New York, 1988).

<sup>18</sup> E. Meyer, H. Heinzlmann, D. Brodbeck, G. Overney, R. Overney, L. Howald, H. Hug, T. Jung, H.-R. Hidber, and H.-J. Güntherodt, *J. Vac. Sci. Technol. B* **9**, 1329 (1991).

<sup>19</sup> See, for example, J.B. Pethica and A.P. Sutton, *J. Vac. Sci. Technol. A* **6**, 2490 (1988); R.J. Colton, S.M. Baker, R.J. Driscoll, M.G. Youngquist, J. Baldeschwiler, and W.J. Kaiser, *ibid.* **6**, 349 (1988).

<sup>20</sup> J.J. Gilman and W.G. Johnston, *Solid State Phys.* **13**, 147 (1962).

<sup>21</sup> Meanwhile, we also have achieved atomic-scale resolution at monatomic steps of NaCl(001) with uncoated silicon tips. The estimated tip radius is of the same order of magnitude.

<sup>22</sup> C. Girard, D. Van Labeke, and J.M. Vigoureux, *Phys. Rev. B* **40**, 12133 (1989).

<sup>23</sup> F.J. Giessibl, *Phys. Rev. B* **45**, 13815 (1992).

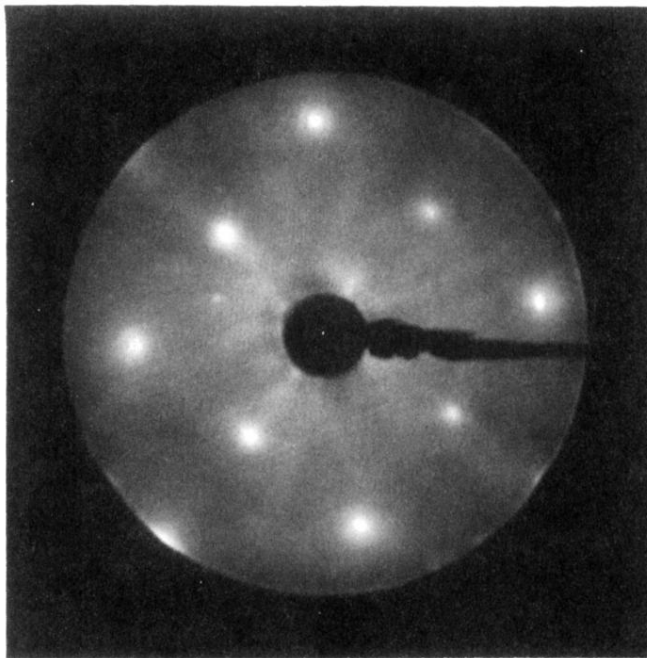


FIG. 1. LEED pattern of NaF(001). Primary electron energy 78 eV.

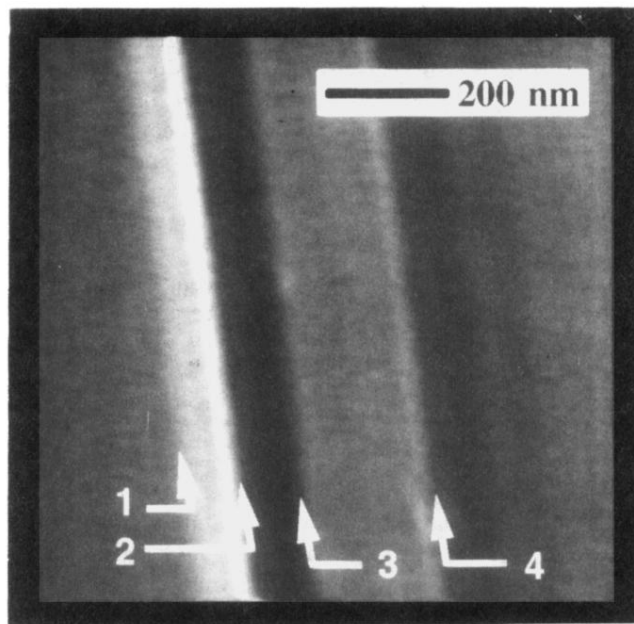


FIG. 2. Force micrograph of a NaF cleavage face on the micrometer scale. The image was taken in the constant force mode. Corresponding to the chosen gray scale, bright regions are assigned high surface features and dark regions low features. The height of several cleavage steps (marked by arrows) were determined to be 0.25 nm (steps 1, 3, and 4) and 0.5 nm (step 2), respectively.



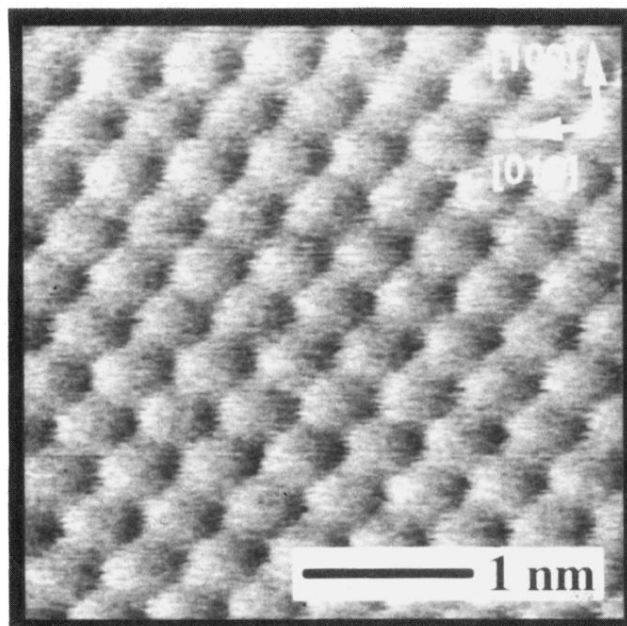


FIG. 3. Atomic-scale resolution on a terrace in the lateral force mode. The spacing between two atomic features (bright spots) in the [010] direction is 0.45 nm and corresponds well to the unit cell length  $a_0$  of 0.463 nm.

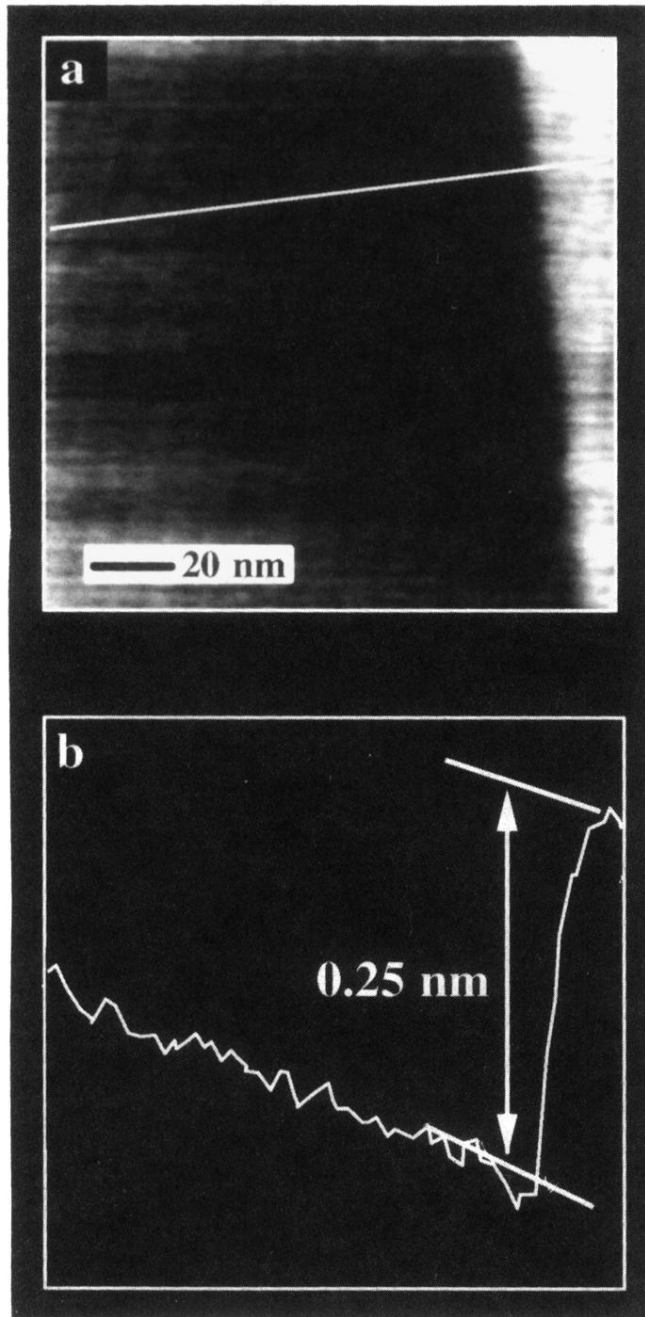


FIG. 4. (a) Topographic image of a monatomic step taken in the constant force mode. (b) The  $z$ -profile analysis (line section) taken along the white line in (a) reveals the step height of 0.25 nm.

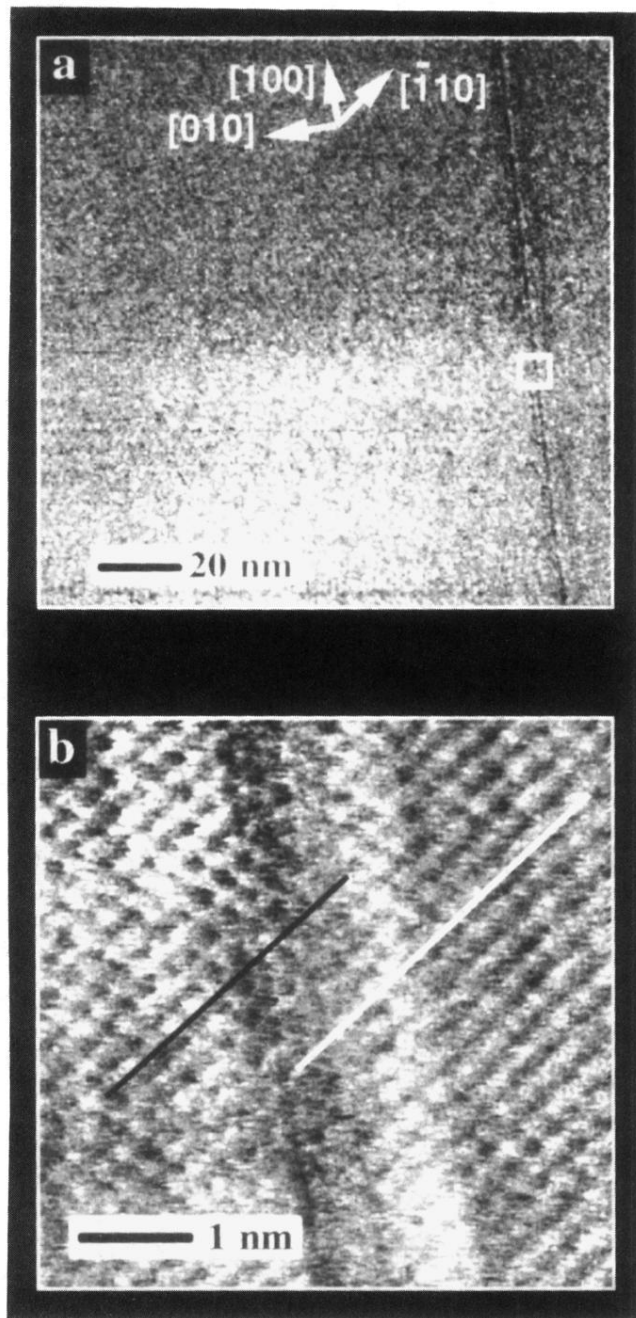


FIG. 5. (a) Lateral force data taken simultaneously with the topographical data of Fig. 4(a). The monatomic step appears here as sharp line. (b) Atomic-scale resolution along this cleavage step in  $5.6 \times 5.6 \text{ nm}^2$  surface area marked by the white frame in (a). The regular lattice patterns are separated by a diffuse region of 0.5 to 1 nm width. The white and black solid lines indicate the shift of atomic rows between adjacent terraces.

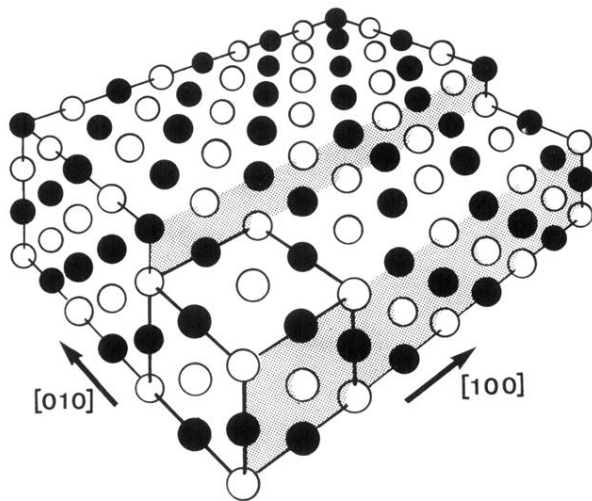


FIG. 6. Perspective view of a terrace-ledge model of a NaCl-type crystal. Both ionic species, represented by open and solid circles, build up two interpenetrating face-centered-cubic lattices. The outline of a single unit cell is indicated by solid lines at the front corner.

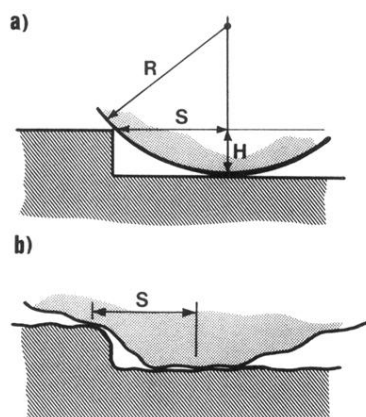


FIG. 7. (a) Idealized tip with a local radius of curvature  $R$  at a step of height  $H$ . For a given separation  $S$  and height  $H$  the radius  $R$  can be calculated. (b) A more realistic tip with a prominent feature and a flat contact area in the nanometer range.

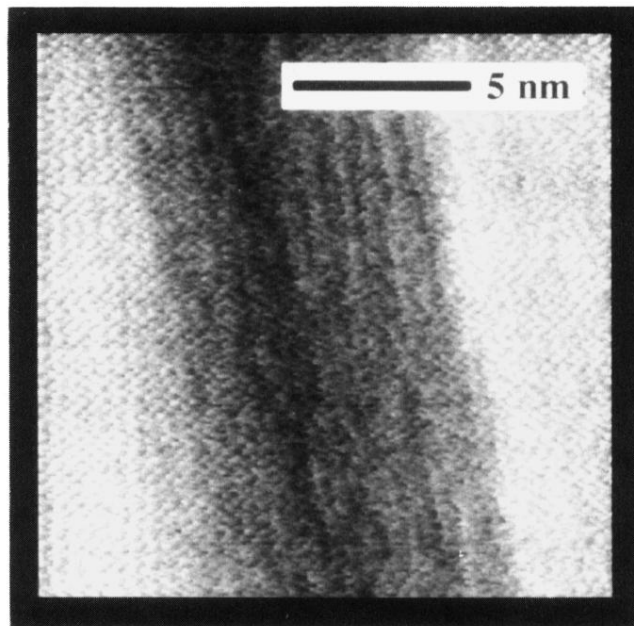


FIG. 8. Lateral force image at the step 2 of Fig. 2. The diffuse region at this 0.5 nm step is about 6 nm wide.